SCIENCE CHINA
Information Sciences

• **Supplementary File** •

One-bit quantization is good for programmable coding metasurfaces

Ya SHUANG †[1], Hanting ZHAO †[1], Menglin WEI[1], Qiang CHENG[2,3,4], Shi JIN[2,3,4], Tie Jun CUI[2,3,4], Philipp DEL HOUGNE[5] & Lianlin LI[6]

[1]*State Key Laboratory of Advanced Optical Communication Systems and Networks,Department of Electronics, Beijing,*100871,*China;*
[2]*Institute of Electromagnetic Space,Southeast University,Nanjing,*210096,*China;*
[3]*State Key Laboratory of Millimeter Waves, Southeast University, Nanjing,*210096,*China;*
[4]*Pazhou Laboratory,Guangzhou,*510330,*China;*
[5]*Univ Rennes,CNRS,IETR-UMR 6164,Rennes,*F-35000,*France*

Appendix A Derivation of Eq. 1

We elaborate on the derivation of **Eq. 1** and provide necessary notations involved. For the SISO setting, the control coding pattern of the one-bit coding metasurface reads

$$\mathcal{C}_{m,n}^{SISO} = \text{sign}\left[\cos\left(\tilde{\phi}_{nm}^{SIIO}\right)\right] \tag{A1}$$

where $\tilde{\phi}_{nm}^{SISO} \equiv \tilde{\phi}_{m,n}\left(\boldsymbol{r}_q;\boldsymbol{r}_s\right), \tilde{\phi}_{m,n}\left(\boldsymbol{r}_q;\boldsymbol{r}_s\right) = \Delta_{m,n}\left(\boldsymbol{r}_q;\boldsymbol{r}_s\right) + \phi\left(\boldsymbol{r}_q\right)$,

$$\Delta_{m,n}\left(\boldsymbol{r}_q;\boldsymbol{r}_s\right) = k(\underbrace{|\boldsymbol{r}_s - \boldsymbol{r}_{m,n}|}_{R_{nm}(r_s)} + \underbrace{|\boldsymbol{r}_q - \boldsymbol{r}_{m,n}|}_{R_{nm}(r_q)}).$$

Herein, $\phi_q \equiv \phi\left(\boldsymbol{r}_q\right)(0 \leqslant \phi_q < 2\pi)$ denotes the intended phase directed from the source to receiver at $\boldsymbol{r}_q$ through the metasurface, and $\text{sign}(x)$ is the sign function:

$$\text{sign}(x) = \begin{cases} +1, x > 0 \\ 0, x = 0 \\ -1, x < 0 \end{cases}$$

Using the following identical equations:

$$\text{sign}(x) = \frac{-j}{\pi}\int_{-\infty}^{\infty}\frac{\exp(jx\xi)}{\xi}d\xi$$
$$\exp\left(j\xi\cos\left(\tilde{\phi}_{nm}\right)\right) = \sum_{p=-\infty}^{\infty}\exp\left(jp\tilde{\phi}_{nm}\right)j^p J_p(\xi)$$

we can express **Eq. A1** as:

$$\mathcal{C}_{m,n}^{SISO} = \frac{-j}{\pi}\int_{-\infty}^{\infty}\frac{1}{\xi}\sum_{p=-\infty}^{\infty}\exp\left(jp\tilde{\phi}_{nm}\right)j^p J_p(\xi)d\xi = \sum_{p=-\infty}^{\infty}B_p^{SISO}\exp\left(jp\tilde{\phi}_{nm}\right) \tag{A2}$$

where $B_p^{SISO} = \frac{-j^{p+1}}{\pi}\int_{-\infty}^{\infty}\frac{1}{\xi}J_p(\xi)d\xi = \frac{-j^{p+1}}{\pi}\int_{-\infty}^{\infty}\frac{1}{\xi}J_p(\xi)d\xi = \begin{cases}\frac{-j^{p+1}}{\pi}\cdot\frac{2}{p}, & p \text{ is odd} \\ 0, & \text{else}\end{cases}$. Now we can derive the radiation response of the one-bit coding metasurface as:

* Corresponding author (email: tjcui@seu.edu.cn, philipp.del-hougne@univ-rennes1.fr, lianlin.li@pku.edu.com)
† Shuang Y and Zhao H T have the same contribution to this work.

$$
\begin{aligned}
\widehat{\mathcal{H}}_{\mathrm{SISO}}\left(\mathbf{r},\mathbf{r}';q,s\right) &= \sum_{m,n}\mathcal{C}_{m,n}^{SISO}\cdot\frac{\exp\left[-j\Delta_{nm}\left(r;\mathbf{r}'\right)\right)]}{R_{nm}(\mathbf{r})R_{nm}\left(\mathbf{r}'\right)} \\
&= \sum_{p=-\infty}^{\infty}B_1^{SISO}\exp\left(jp\phi_q\right)\sum_{m,n}\frac{\exp\left[jp\Delta_{m,n}\left(r_q;r_s\right)-j\Delta_{nm}\left(r;r'\right)\right)]}{R_{nm}(r)R_{nm}\left(r_s\right)} \\
&= B_1^{SISO}\exp\left(j\phi_q\right)\underbrace{\sum_{m,n}\frac{\exp\left[j\Delta_{m,n}\left(r_q;r_s\right)-j\Delta_{nm}\left(r;\mathbf{r}'\right)\right)]}{R_{nm}(r)R_{nj}\left(\mathbf{r}'\right)}}_{A_1^{SISO}\left(r,r';q,q\right)} \\
&+ \sum_{p=-\infty,p\neq1}^{\infty}B_p^{SISO}\exp\left(jp\phi_q\right)\underbrace{\sum_{m,n}\frac{\exp\left[jp\Delta_{m,n}\left(r_q;r_s\right)-j\Delta_{nm}\left(r;\mathbf{r}'\right)\right)]}{R_{nm}\left(r_n\right)}}_{A_p^{SISO}\left(r,r';q,s'\right)}
\end{aligned}
\tag{A3}
$$

where $\sum_{m,n}\equiv\sum_{n=1}^{N}\sum_{m=1}^{M}$. After introducing the following notations

$$
\begin{aligned}
E_1^{SISO}\left(\boldsymbol{r},\mathbf{r}';q,s\right) &= B_1^{SISO}\exp\left(j\phi_q\right)A_1^{SISO}\left(\boldsymbol{r},\mathbf{r}';q,s\right) \\
A_p^{SISO}\left(\boldsymbol{r},\mathbf{r}';q,s\right) &= \sum_{m,n}\frac{\exp\left[jp\Delta_{m,n}\left(r_q;\boldsymbol{r}_s\right)-j\Delta_{nm}\left(r;\mathbf{r}'\right)\right)]}{R_{nm}(\boldsymbol{r})R_{nm}\left(\mathbf{r}'\right)},
\end{aligned}
$$

then the proof of **Eq.1** in main text can be readily completed:

$$
\widehat{\mathcal{H}}_{\mathrm{SISO}}\left(\mathbf{r},\mathbf{r}';q,s\right)=\underbrace{E_1^{\mathrm{SISO}}\left(\boldsymbol{r},\mathbf{r}';q,s\right)}_{\text{leading term}}+\underbrace{\sum_{p=-\infty,p\neq1}^{\infty}B_p^{SISO}A_p^{\mathrm{SISO}}\left(\boldsymbol{r},\mathbf{r}';q,s\right)\exp\left(jp\phi_q\right)}_{\text{perturbation terms}}
\tag{A4}
$$

Discussion 1. The derivation of $A_p=\frac{-j^{p+1}}{\pi}\int_{-\infty}^{\infty}\frac{1}{\xi}J_p(\xi)d\xi$.

We focus on the derivation of $A_p=\frac{-j^{p+1}}{\pi}\int_{-\infty}^{\infty}\frac{1}{\xi}J_p(\xi)d\xi$. It can be processed as

$$
A_p=\frac{-j^{p+1}}{\pi}\int_{-\infty}^{\infty}\frac{1}{\xi}J_p(\xi)d\xi=\begin{cases}2\frac{-j^{p+1}}{\pi}\int_0^{\infty}\frac{1}{\xi}J_p(\xi)d\xi, & p\text{ is odd}\\ 0, & \text{else}\end{cases}=\begin{cases}-\frac{2}{p}\frac{j^{p+1}}{\pi}, & p\text{ is odd}\\ 0, & \text{is else}\end{cases}
\tag{A5}
$$

in which we have used a fundamental property of the Bessel function

$$
J_p(-\xi)=(-1)^pJ_p(\xi)=J_{-p}(\xi)
$$

and the integral identical equation of the Bessel function

$$
\int_0^{\infty}\frac{1}{\xi}J_p(\xi)d\xi=\frac{1}{2}\frac{\Gamma\left(\frac{p}{2}\right)}{\Gamma\left(\frac{p}{2}+1\right)}=\frac{1}{p}\text{ if }p>0.
$$

Discussion 2. Far-field solution of **Eq.A4**.

We study the system response $\widehat{\mathcal{H}}_{\mathrm{SISo}}$ when the source and receiver are in the far-field region of the one-bit coding metasurface. For this purpose, we would like to consider the calculation of $A_p^{SISO}\left(\boldsymbol{r},\boldsymbol{r}';q,s\right)$ in the spherical coordinate system. To this end, some necessary notations are introduced as follows:

$$
\begin{aligned}
&\hat{\boldsymbol{r}}_q=\hat{\boldsymbol{x}}\sin\left(\alpha_q\right)\cos\left(\beta_q\right)+\hat{\boldsymbol{y}}\sin\left(\alpha_q\right)\sin\left(\beta_q\right)+\hat{\mathbf{z}}\cos\left(\alpha_q\right),\\
&\hat{\boldsymbol{r}}_s=\hat{\boldsymbol{x}}\sin\left(\alpha_s\right)\cos\left(\beta_s\right)+\hat{\boldsymbol{y}}\sin\left(\alpha_s\right)\sin\left(\beta_s\right)+\hat{\mathbf{z}}\cos\left(\alpha_s\right),\\
&\hat{\boldsymbol{r}}=\hat{\boldsymbol{x}}\sin(\alpha)\cos(\beta)+\hat{\mathbf{y}}\sin(\alpha)\sin(\beta)+\hat{\mathbf{z}}\cos(\alpha),\\
&\hat{\mathbf{r}}'=\hat{\boldsymbol{x}}\sin\left(\alpha'\right)\cos\left(\beta'\right)+\widehat{\boldsymbol{y}}\sin\left(\alpha'\right)\sin\left(\beta'\right)+\hat{\mathbf{z}}\cos\left(\alpha'\right)\\
&\boldsymbol{r}_{m,n}\cdot\left(\hat{\boldsymbol{r}}_q+\hat{\boldsymbol{r}}_s\right)=x_m\left[\sin\left(\alpha_q\right)\cos\left(\beta_q\right)+\sin\left(\alpha_s\right)\cos\left(\beta_s\right)\right]+\\
&y_n\left[\sin\left(\alpha_q\right)\sin\left(\beta_q\right)+\sin\left(\alpha_s\right)\sin\left(\beta_s\right)\right],\\
&\boldsymbol{r}_{m,n}\cdot\left(\hat{\boldsymbol{r}}+\hat{\boldsymbol{r}}'\right)=x_m\left[\sin(\alpha)\cos(\beta)+\sin\left(\alpha'\right)\cos\left(\beta'\right)\right]\\
&+y_n\left[\sin(\alpha)\sin(\beta)+\sin\left(\alpha'\right)\sin\left(\beta'\right)\right],\\
&\xi_p^{SISO}=\sin(\alpha)\cos(\beta)+\sin\left(\alpha'\right)\cos\left(\beta'\right)-p\left[\sin\left(\alpha_q\right)\cos\left(\beta_q\right)+\sin\left(\alpha_s\right)\cos\left(\beta_s\right)\right],\\
&\eta_p^{SISO}=\sin(\alpha)\sin(\beta)+\sin\left(\alpha'\right)\sin\left(\beta'\right)-p\left[\sin\left(\alpha_q\right)\sin\left(\beta_q\right)+\sin\left(\alpha_s\right)\sin\left(\beta_s\right)\right].
\end{aligned}
$$

Then, $A_p^{SISO}\left(\boldsymbol{r},\boldsymbol{r}';q,s\right)$ under the far-field approximation can be derived as:

$$
\begin{aligned}
A_p^{SISO}\left(\boldsymbol{r},\boldsymbol{r}';q,s\right) &= \sum_{m,n}\frac{\exp\left[jp\Delta_{m,n}\left(r_q;\boldsymbol{r}_s\right)-j\Delta_{nm}\left(r;\mathbf{r}'\right)\right)]}{R_{nm}(\boldsymbol{r})R_{nm}\left(\mathbf{r}'\right)}\\
&\approx\frac{\exp\left[jkp\left(r_q+r_s\right)-j\left(\left(r+r'\right)\right)\right]}{rr\prime}\sum_{m,n}\exp\left[-jkp\boldsymbol{r}_{m,n}\cdot\left(\hat{\boldsymbol{r}}_q+\hat{\boldsymbol{r}}_s\right)+jk\boldsymbol{r}_{m,n}\cdot\left(\hat{\boldsymbol{r}}+\hat{\boldsymbol{r}}'\right)\right]\\
&\approx-\frac{\exp\left[jkp\left(r_q+r_s\right)-j\left(\left(r+r'\right)\right)\right]}{rr}L_xL_y\operatorname{sinc}\left(\frac{1}{2}kL_x\xi_p^{SISO}\right)\operatorname{sinc}\left(\frac{1}{2}kL_y\eta_p^{SISO}\right)
\end{aligned}
\tag{A6}
$$

Here, L_x and L_y denote the scales of metasurface along the x - and y-directions, respectively; $\mathrm{sinc}(x) = \frac{\sin(x)}{x}$ has been defined; and the following approximation has been used

$$\Delta_{m,n}\left(\boldsymbol{r};\boldsymbol{r}'\right) = k\left(\left|\boldsymbol{r}'-\boldsymbol{r}_{m,n}\right| + \left|\boldsymbol{r}-\boldsymbol{r}_{m,n}\right|\right) \approx k\left(r'+r-\boldsymbol{r}_{m,n}\cdot\left(\hat{\boldsymbol{r}}+\hat{\boldsymbol{r}}'\right)\right) \tag{A7}$$

Using **Eq.A7** in **Eq.A4** immediately leads to the far-field expression of the system response for the SISO setting.

It is clear from **Eq.A6** that if the vector of $\hat{\boldsymbol{r}}+\hat{\boldsymbol{r}}'+\hat{\boldsymbol{r}}_q+\hat{\boldsymbol{r}}_s$ is along with the normal direction of the metasurface, then we have $\left|A_{-1}^{\mathrm{SIIO}}\right| = \left|A_1^{\mathrm{SISO}}\right|$. Recall that $B_{-1}^{\mathrm{SISO}} = B_1^{\mathrm{SISO}}$, we can arrive at the following conclusion: When the source and intended receiver are in the far-field region of the metasurface, the one-bit quantization of the metasurface can give rise to an unwanted dominant parasitic radiation beam

$$E_{\mathrm{parasite}}^{\mathrm{SISO}}\left(\boldsymbol{r},\mathbf{r}';q,s\right) = B_1^{\mathrm{SISO}}\exp\left(-j\phi_q\right)A_{-1}^{\mathrm{SISO}}\left(\boldsymbol{r},\mathbf{r}';q,s\right).$$

Note that this parasitic beam has the same maximum intensity as the desired radiation beam E_1^{SISO} but with different radiation phase shift $\exp\left(-j\phi_q\right)$. Please see more details about the parasitic radiation beams below.

Discussion 3. Parasitic radiation beams of the one-bit coding metasurface

We provide some insights into the parasitic radiation beams when the receiver and source fall into the far-field region of the one-bit coding metasurface. For convenience of discussion, we denote the location of the (m, n) meta-atom in the rectangular coordinate system by $\boldsymbol{r}_{m,n} = (nd_x, md_y, 0)$, where d_x and d_y are the scales of the meta-atom along the x - and y - directions, respectively. In term of the paraxial approximation, we have

$$\left|\boldsymbol{r}-\boldsymbol{r}_{m,n}\right| \approx z + \frac{\rho^2+\rho_{mn}^2-2\left(nd_x\rho_x+md_y\rho_y\right)}{2z} \tag{A8}$$

Herein, $r = (\rho_x,\rho_y,z)$, $\rho^2 = \rho_x^2+\rho_y^2$ and $\rho_{mn}^2 = (nd_x)^2+(md_y)^2$. Note that one of the critical issues for calculating A_p^{SISO} is to deal with $p\Delta_{nm}\left(\boldsymbol{r}_q;\boldsymbol{r}_s\right)-\Delta_{nm}\left(\boldsymbol{r};\boldsymbol{r}'\right)$. To that end, we apply the paraxial approximation to $\Delta_{nm}\left(\boldsymbol{r};\boldsymbol{r}'\right)$ and $\Delta_{nm}\left(\boldsymbol{r}_q;\boldsymbol{r}_s\right)$, in particular,

$$\begin{aligned}\Delta_{nm}\left(\boldsymbol{r};\boldsymbol{r}'\right) &= k\left|\boldsymbol{r}'-\boldsymbol{r}_{m,n}\right| + k\left|\boldsymbol{r}-\boldsymbol{r}_{m,n}\right| \\ &\approx k\left(z'+z\right) + k\frac{\rho'^2+\rho_{mn}^2-2\left(nd_x\rho_x'+md_y\rho_y'\right)}{2z\prime} + k\frac{\rho^2+\rho_{mn}^2-2\left(nd_x\rho_x+md_y\rho_y\right)}{2z}\end{aligned} \tag{A9}$$

and

$$\begin{aligned}\Delta_{nm}\left(\boldsymbol{r}_q;\boldsymbol{r}_s\right) &= k\left|\boldsymbol{r}_s-\boldsymbol{r}_{m,n}\right| + k\left|\boldsymbol{r}_q-\boldsymbol{r}_{m,n}\right| \\ &\approx k\left(z_s+z_q\right) + k\frac{\rho_s^2+\rho_{mn}^2-2\left(nd_x\rho_{sx}+md_y\rho_{sy}\right)}{2z_s} + k\frac{\rho_q^2+\rho_{mn}^2-2\left(nd_x\rho_{qx}+md_y\rho_{qy}\right)}{2z_q}.\end{aligned} \tag{A10}$$

Then, $p\Delta_{nm}\left(\boldsymbol{r}_q;\boldsymbol{r}_s\right)-\Delta_{nm}\left(\boldsymbol{r};\boldsymbol{r}'\right)$ becomes:

$$\begin{aligned}&p\Delta_{nm}\left(\boldsymbol{r}_q;\boldsymbol{r}_s\right)-\Delta_{nm}\left(\boldsymbol{r};\boldsymbol{r}'\right) = pk\frac{\rho_{mn}^2-2\left(nd_x\rho_{sx}+md_y\rho_{sy}\right)}{2z_s} + pk\frac{\rho_{mn}^2-2\left(nd_x\rho_{qx}+md_y\rho_{qy}\right)}{2z_q} \\ &-k\frac{\rho_{mn}^2-2\left(nd_x\rho_x'+md_y\rho_y'\right)}{2z'} - k\frac{\rho_{mn}^2-2\left(nd_x\rho_x+md_y\rho_y\right)}{2z} + k\cdot\varepsilon^{SISO} \\ &= -\frac{k}{2z}\underbrace{\left(1+\frac{z}{z'}-p\frac{z}{z_s}-p\frac{z}{z_q}\right)}_{\beta^{SISO}}\rho_{mn}^2 + \underbrace{\left(\rho_x+\frac{z}{z'}\rho_x'-\frac{z}{z_s}p\rho_{sx}-\frac{z}{z_q}p\rho_{qx}\right)}_{\frac{k}{z}}nd_x \\ &+\frac{k}{z}\underbrace{\left(\rho_y+\frac{z}{z'}\rho_y'-\frac{z}{z_s}p\rho_{sy}-\frac{z}{z_q}p\rho_{qy}\right)}_{b_y^{SISO}}md_y + k\cdot\mathcal{E}^{SISO}\end{aligned} \tag{A11}$$

Herein, $\mathcal{E}^{\mathrm{SISO}} = p\left(z_s+z_q\right)-\left(z'+z\right)+p\left(\frac{\rho_S^2}{2z_s}+\frac{\rho_q^2}{2z_q}\right)-\left(\frac{\rho'^2}{2z'}+\frac{\rho^2}{2z}\right)$, $\boldsymbol{r}_s = (\rho_{sx},\rho_{sy},z_s)$ $\rho_s^2 = \rho_{sx}^2+\rho_{sy}^2$, $\boldsymbol{r}_q = (\rho_{qx},\rho_{qy},z_q)$, $\rho_q^2 = \rho_{qx}^2+\rho_{qy}^2$. Substituting **Eq. A11** into $A_p^{SISO}\left(\boldsymbol{r},\boldsymbol{r}';q,s\right)$, leads to:

$$\begin{aligned}A_p^{SISO}\left(\boldsymbol{r},\boldsymbol{r}';q,S\right) &= \sum_{m,n}\frac{\exp\left[j\left(p\Delta_{nm}\left(\boldsymbol{r}_q;\boldsymbol{r}_S\right)-\Delta_{nm}\left(\boldsymbol{r};\boldsymbol{r}'\right)\right)\right]}{R_{nm}(\boldsymbol{r})R_{nm}(\boldsymbol{r}\prime)} \\ &\approx \frac{1}{zZ'}\frac{\pi}{\alpha+i\frac{k\beta^{SISO}}{2z}}\exp\left(-\frac{k^2}{4z^2}\frac{\left(b_x^{SISO}\right)^2+\left(b_y^{SISO}\right)^2}{\alpha+i\frac{k\beta^{SISO}}{2z}}\right)\exp\left(jk\mathcal{E}^{SISO}\right)\end{aligned} \tag{A12}$$

In the second line of **Eq**.**A12**, we have assumed the Gaussian illumination beam of the source, and the beam width is $\alpha = (Nd_x/2)^{-2}$. In addition, the following integral identical equation has been used

$$\int_{-\alpha}^{\alpha}\exp\left(-\alpha t^2+j\beta t^2+jbt\right)dt = \sqrt{\frac{\pi}{\alpha-i\beta}}\exp\left(-\frac{b^2}{4(\alpha-i\beta)}\right)$$

It is clear from Eq. A12 that the parasitic beams of the one-bit coding metasurface can be observed at $(\rho_x(p),\rho_y(p),z)$ $(p = -1,\pm3,\pm5,\ldots)$, where ρ_x and ρ_y are defined as

$$\rho_x(p,z) = \frac{z}{z_s}p\rho_{sx}+\frac{z}{z_q}p\rho_{qx}-\frac{z}{z'}\rho_x' \tag{A13}$$

$$\rho_y(p,z) = \frac{z}{z_s}p\rho_{sy}+\frac{z}{z_q}p\rho_{qy}-\frac{z}{z'}\rho_y' \tag{A14}$$

Appendix B Some details about Fig. 2

We here provide details about $\left|E_p^{\mathrm{SISO}}\right|$ involved in Fig. 2 in the main text. **Fig. B1** plots the spatial maps of $\left|\widehat{\mathcal{H}}_{\mathrm{SISO}}\right|$ corresponding to **Fig. 2** in the main text. In order to show details of $\left|E_p^{\mathrm{SISO}}\right|$, the first a few non-zero terms $\left|E_p^{SISO}\right|$ are normalized by their maximum. From these figures, we can verify two findings made in the main text, i.e., 1) the quantization energy loss is statistically uniformly distributed over the entire space when the receiver or/and source is in the near-field region of the metasurface; and 2) multiple unwanted parasitic beams appear that interfere with the desired beam when the receiver and source are in the far-field region of the one-bit coding metasurface.

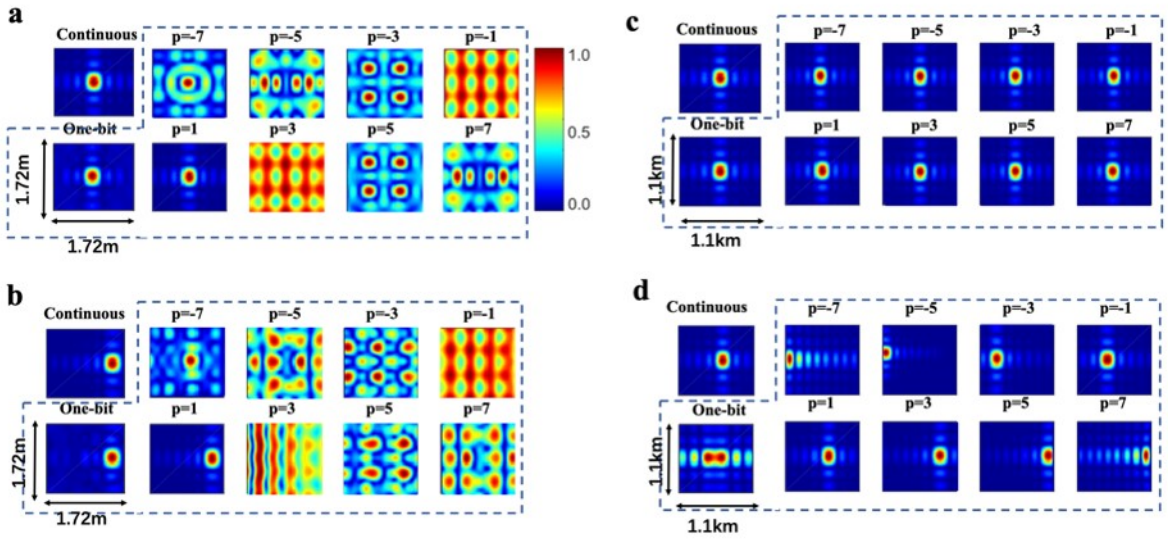

Figure B1 Spatial maps of $\left|\widehat{\mathcal{H}}_{\mathrm{SISO}}\right|$ for continuous and one-bit coding metasurfaces. The simulation setup and notations are the same as those in Fig.2 in main text, but the maps of $\left|E_p^{SISO}\right|$ are normalized by their own maximum.

Appendix C Derivation of Eq. 7

We elaborate on the derivation of **Eq.7** in the main text. For the SIMO setting, the control coding pattern of the one-bit coding metasurface reads

$$\mathcal{C}_{m,n}^{SIMO} = \mathrm{sign}\left[\sum_{q=1}^{Q}\cos\left(\tilde{\phi}_{nm}^{SIMO}(q)\right)\right] \tag{C1}$$

where $\tilde{\phi}_{nm}^{SIMO}(q) \equiv \tilde{\phi}_{m,n}\left(\boldsymbol{r}_q;\boldsymbol{r}_s\right)$, $\tilde{\phi}_{m,n}\left(\boldsymbol{r}_q;\boldsymbol{r}_s\right) = \Delta_{m,n}\left(\boldsymbol{r}_q;\boldsymbol{r}_s\right)+\phi_q$, and $\Delta_{m,n}\left(\boldsymbol{r}_q;\boldsymbol{r}_s\right) = k(\underbrace{|\boldsymbol{r}_s-\boldsymbol{r}_{m,n}|}_{R_{nm}(r_s)}+\underbrace{|\boldsymbol{r}_q-\boldsymbol{r}_{m,n}|}_{R_{nm}(r_q)})$. Similar to those in Appendix A, we express **Eq. C1** as:

$$\begin{aligned}
\mathcal{C}_{m,n}^{SIMO} &= \mathrm{sign}\left[\sum_{q=1}^{Q}\cos\left(\tilde{\phi}_{nm}^{SIMO}(q)\right)\right] = \frac{-j}{\pi}\int_{-\infty}^{\infty}\frac{1}{\xi}\prod_{q=1}^{Q}\exp\left[j\xi\cos\left(\tilde{\phi}_{nm}(q)\right)\right]d\xi \\
&= \frac{-j}{\pi}\int_{-\infty}^{\infty}\frac{1}{\xi}\sum_{p_1}\sum_{p_2}\cdots\sum_{p_Q}\exp\left(j\sum_{q}p_q\tilde{\phi}_{nm}(q)\right)j^{\sum_q p_q}\prod_{q=1}^{Q}J_{p_q}(\xi)d\xi \\
&= \sum_{p_1}\sum_{p_2}\cdots\sum_{p_Q}\exp\left(j\sum_{q}p_q\tilde{\phi}_{nm}(q)\right)\int_{-\infty}^{\infty}\frac{-j}{\pi}j^{2\Sigma_q p_q}\frac{1}{\xi}\prod_{q=1}^{Q}J_{p_q}(\xi)d\xi
\end{aligned} \tag{C2}$$

in which, $\sum_{p_i} \equiv \sum_{p_i=-\infty}^{\infty}$ and $\sum_q \equiv \sum_{q=1}^{Q}$. After introducing the notations $B_{\{p_i\}}^{SMO} \equiv \frac{-j}{\pi}j^{\Sigma_q p_q}\int_{-\infty}^{\infty}\frac{1}{\xi}\Pi_{q=1}^{Q}J_{p_q}(\xi)d\xi$ and $\Sigma_{\{p_i\}} \equiv \sum_{p_1}\Sigma_{p_2}\cdots\Sigma_{p_Q}$, we can express **Eq.C2** as:

$$\mathcal{C}_{m,n}^{SIMO} = \sum_{\{p_i\}}B_{\{p_i\}}^{SIMO}\exp\left(j\sum_{q}p_q\tilde{\phi}_{nm}(q)\right) \tag{C3}$$

Now, we can arrive at the SIMO's system response of the one-bit coding metasurface as

$$\begin{aligned}
&\widehat{\mathcal{H}}_{\text{SIMO}}\ (\mathbf{r},\mathbf{r}';\{q\},s)=\sum_{m,n}\mathcal{C}_{m,n}^{SIMO}\frac{\exp\left[-j\Delta_{nm}\left(r;\mathbf{r}'\right)\right)]}{R_{nm}(r)R_{nm}\left(\mathbf{r}'\right)}\\
&=\sum_{\{p_i\}}\exp\left(j\sum_q p_q\phi_q\right)B_{\{p_i\}}^{\text{SIMO}}\underbrace{\sum_{m,n}\frac{\exp\left[j\Sigma_q p_q\Delta_{m,n}\left(r_q;\boldsymbol{r}_s\right)-j\Delta_{nm}\left(r;\mathbf{r}'\right)\right)]}{R_{nm}(r)r_{nm})}}_{A_{\{p_i\}}^{SIM}(r,\mathbf{r}')}\\
&=\underbrace{B_1^{\text{SIMO}}\sum_{q=1}^{Q}\exp\left(j\phi_q\right)A_1^{SISO}\left(\boldsymbol{r},\mathbf{r}';q,s\right)}_{E_1^{SIMO}(r,\mathbf{r}';\{q\},s)}+\\
&+\underbrace{\sum_{\{p_i\}/\{\sum_i|p_i|=1\&p_i\neq-1\}}E_{\{p_{ij}\}}^{SIMO}\left(\boldsymbol{r},\mathbf{r}';\{q\},s\right)\exp\left[j\sum_{q=1}^{Q}p_q\phi_q\right]}_{\text{perturbation terms}}
\end{aligned}\tag{C4}$$

Herein, $B_1^{SIMO}=\frac{1}{\pi}\int_{-\infty}^{\infty}\frac{1}{\xi}J_1(\xi)J_0^{Q-1}(\xi)d\xi$, and $E_{\{p_{ij}\}}^{SIMO}\left(\boldsymbol{r},\mathbf{r}';\{q\},s\right)=B_{\{p_i\}}^{SIMO}A_{\{p_i\}}^{SIMO}\left(\boldsymbol{r},\mathbf{r}'\right)$. In addition, the operator denoted by $\sum_{\{p_i\}/\{\sum_i|p_i|=1\&p_i\neq-1\}}$ is defined as follows. For a function of $f\left(p_1,p_2,\ldots,p_Q\right)$, we define:

$$\sum_{\{p_i\}/\{\sum_i|p_i|=1\&p_i\neq-1\}}f\left(p_1,p_2,\ldots,p_Q\right)=\sum_{\{p_i\}}f\left(p_1,p_2,\ldots,p_Q\right)-\left[f(1,0,0,\ldots,0)+f(0,1,0,\ldots,0)+\cdots+f(0,0,0,\ldots,1)\right]$$

Discussion 1. The derivation of $B_{\{p_1,p_2\}}^{SIMO}=\frac{-jp_1+p_2+1)}{\pi}\int_{-\infty}^{+\infty}\frac{J_{p_1}(\xi)p_{p_2}(\xi)}{\xi}d\xi$.

We consider the calculation of $B_{\{p_i\}}^{SIMO}$ for the special SIMO case: single-input double-output, Q=2. Then, we deal with $B_{\{p_1,p_2\}}^{SIMO}=\frac{-j(p_1+p_2+1)}{\pi}\int_{-\infty}^{+\infty}\frac{J_{p_1}(\xi)J_{p_2}(\xi)}{\xi}d\xi$ as follows:

$$\begin{aligned}
B_{\{p_1,p_2\}}^{\text{SIMO}}&=\frac{-j^{(p_1+p_2+1)}}{\pi}\int_{-\infty}^{+\infty}\frac{J_{p_1}(\xi)J_{p_2}(\xi)}{\xi}d\xi\\
&=\frac{-jp_1+p_2+1)}{\pi}\cdot\frac{2}{\pi}\int_{-\infty}^{\infty}\int_0^{\frac{\pi}{2}}\frac{J_{p_1+p_2}(2x\cos\theta)\cos\left[\left(p_1-p_2\right)\theta\right]}{\xi}d\theta d\xi\\
&=\frac{-j^{(p_1+p_2+1)}}{\pi}\cdot\frac{2}{\pi}\int_0^{\frac{\pi}{2}}\cos\left[\left(p_1-p_2\right)\theta\right]\left[\int_{-\infty}^{\infty}\frac{J_{p_1+p_2}(2x\cos\theta)}{\xi}d\xi\right]d\theta\\
&=\frac{-j^{(p_1+p_2+1)}}{\pi}\cdot\frac{2}{\pi}\cdot\frac{2}{p_1+p_2}\int_0^{\frac{\pi}{2}}\cos\left[\left(p_1-p_2\right)\theta\right]d\theta\\
&=\frac{-j\left(p_1+p_2+1\right)}{p_1+p_2}\cdot\left(\frac{2}{\pi}\right)^2\cdot\frac{\sin\left[\left(p_1-p_2\right)\frac{\pi}{2}\right]}{p_1-p_2}
\end{aligned}\tag{C5}$$

In the first and fourth lines of **Eq. C5**, the following identical equations

$$\begin{aligned}
&J_{p_1}(x)J_{p_2}(x)=\frac{2}{\pi}\int_0^{\frac{\pi}{2}}J_{p_1+p_2}(2x\cos\theta)\cos\left[\left(p_1-p_2\right)\theta\right]d\theta,\\
&\int_{-\infty}^{\infty}\frac{J_{p_1+p_2}(2\xi\cos\theta)}{\xi}d\xi=\begin{cases}0, & p_1+p_2\text{ is even}\\ \frac{2}{p_1+p_2}, & p_1+p_2i\text{ is odd}\end{cases}
\end{aligned}$$

have been used, respectively. Finally, we can arrive at the closed-form solution of $B_{\{p_1,p_2\}}^{SIO}$ as

$$B_{\{p_1,p_2\}}^{SIMO}=\begin{cases}0, & p_1+p_2\text{ is even}\\ \frac{-j(p_1+p_2+1)}{p_1+p_2}\cdot\left(\frac{2}{\pi}\right)^2\cdot\frac{\sin\left[\left(p_1-p_2\right)\frac{\pi}{2}\right]}{p_1-p_2}, & p_1+p_2\text{ is odd}\end{cases}\tag{C6}$$

Especially, the leading term is $B_0^{SIMO}=\frac{2}{\pi}\int_0^{\infty}\frac{1}{\xi}J_0(\xi)J_1(\xi)d\xi=\left(\frac{2}{\pi}\right)^2$.

Discussion 2. Parasitic radiation beams of the one-bit coding metasurface

We here provide some insights into the parasitic radiation beams when the source and multiple intended receivers are deployed

in the far-field region of the one-bit coding metasurface. Similar to above, we treat $\sum_q p_q \Delta_{nm}\left(\boldsymbol{r}_q;\boldsymbol{r}_s\right)-\Delta_{nm}\left(\boldsymbol{r};\boldsymbol{r}'\right)$ as follows:

$$\begin{aligned}\sum_q p_q \Delta_{nm}\left(\boldsymbol{r}_q;\boldsymbol{r}_s\right)-\Delta_{nm}\left(\boldsymbol{r};\boldsymbol{r}'\right)=&-\frac{k}{2z}\underbrace{\left(1+\frac{z}{z'}-\sum_q p_q\left(\frac{z}{z_s}+\frac{z}{z_q}\right)\right)}_{\beta^{\mathrm{SIMO}}}\rho_{mn}^2\\&+\frac{k}{z}\underbrace{\left(\rho_x+\frac{z}{z'}\rho_x'-\sum_q p_q\left(\frac{z}{z_s}\rho_{sx}+\frac{z}{z_q}\rho_{qx}\right)\right)}_{b_x^{\mathrm{SIMO}}}nd_x\\&+\frac{k}{z}\underbrace{\left(\rho_y+\frac{z}{z'}\rho_y'-\sum_q p_q\left(\frac{z}{z_s}\rho_{sy}+\frac{z}{z_q}\rho_{qy}\right)\right)}_{b_y^{\mathrm{SIMO}}}md_y+k\mathcal{E}^{\mathrm{SIMO}}\end{aligned}$$

Herein, $\varepsilon^{SIMO}=p\left(z_s+z_q\right)-\left(z'+z\right)+\sum_q p_q\left(\frac{\rho_s^2}{2z_s}+\frac{\rho_q^2}{2z_q}\right)-\left(\frac{\rho'^2}{2z'}+\frac{\rho^2}{2z}\right)$. Along the same line as that used in **Appendix A**, we can arrive at the close-form solution to $A_{\{p_i\}}^{SMO}\left(\boldsymbol{r},\boldsymbol{r}';\{q\},s\right)$:

$$\begin{aligned}A_{\{p_i\}}^{\mathrm{SIMO}}\left(\boldsymbol{r},\boldsymbol{r}';\{q\},s\right)&=\sum_{m,n}\frac{\exp\left(j\left[\sum_{q=1}^{Q}p_q\Delta_{m,n}\left(r_q;r_s\right)-\Delta_{m,n}\left(r;rr'\right)\right]\right)}{R_{nm}(\boldsymbol{r})R_{nm}\left(r'\right)}\\&\approx\frac{1}{zz\prime}\frac{\pi}{\alpha+i\frac{k\beta^{\mathrm{SIMO}}}{2z}}\exp\left(-\frac{k^2}{4z^2}\frac{\left(b_x^{\mathrm{SIMO}}\right)^2+\left(b_y^{\mathrm{SIMO}}\right)^2}{\alpha+i\frac{k\beta^{\mathrm{SIMO}}}{2z}}\right)\exp\left(jk\mathcal{E}^{\mathrm{SIMO}}\right).\end{aligned}\tag{C7}$$

Then, for the SIMO setting, the parasitic radiation beams can be observed at the locations of $\left(\rho_x\left(\{p_q\}\right),\rho_y\left(\{p_q\}\right),z\right)$, where $\rho_x\left(\{p_q\}\right)=\sum_q p_q\left(\frac{z}{z_s}\rho_{sx}+\frac{z}{z_q}\rho_{qx}\right)-\frac{z}{z'}\rho_x'$, and $\rho_y\left(\{p_q\}\right)=\sum_q p_q\left(\frac{z}{z_s}\rho_{sy}+\frac{z}{z_q}\rho_{qy}\right)-\frac{z}{z'}\rho_y'$.

Discussion 3. Far-field solution of **Eq. C4**

Here, we will study the system response $\widehat{\mathcal{H}}_{\mathrm{SIM}}$ when the source and intended receivers are in the far-field region of the one-bit coding metasurface. Similar to the SISO case discussed in **Appendix A**, we deal with $A_{\{p_i\}}^{SIO}\left(\boldsymbol{r},\boldsymbol{r}';\{q\},s\right)$ as follows

$$\begin{aligned}A_{\{p_i\}}^{SIMO}\left(\boldsymbol{r},\boldsymbol{r}';\{q\},s\right)\approx&\frac{\exp\left[jk\sum_q p_q\left(r_q+r_s\right)-jk\left(\left(r+r'\right)\right)\right]}{rr'}\\&\times\sum_{m,n}\exp\left[-jk\boldsymbol{r}_{m,n}\cdot\sum_q p_q\left(\hat{\boldsymbol{r}}_q+\hat{\boldsymbol{r}}_s\right)+jk\boldsymbol{r}_{m,n}\cdot\left(\hat{\boldsymbol{r}}+\hat{\boldsymbol{r}}'\right)\right]\\\approx&-\frac{\exp\left[jk\sum_q p_q\left(r_q+r_s\right)-jk\left(\left(r+r'\right)\right)\right]}{rr'}\\&\times L_xL_y\,\mathrm{sinc}\left(\frac{1}{2}kL_x\xi^{\mathrm{SIMO}}\left(\{p_i\}\right)\right)\mathrm{sinc}\left(\frac{1}{2}kL_y\eta^{\mathrm{SIMO}}\left(\{p_i\}\right)\right)\end{aligned}\tag{C8}$$

Herein, ξ^{SIMO} and η^{SIMO} are defined as: $\xi^{\mathrm{SIMO}}\left(\{p_i\}\right)=\sin(\alpha)\cos(\beta)+\sin\left(\alpha'\right)\cos\left(\beta'\right)-\sum_q p_q\left[\sin\left(\alpha_q\right)\cos\left(\beta_q\right)+\sin\left(\alpha_s\right)\cos\left(\beta_s\right)\right]$, and $\eta^{\mathrm{SIMO}}\left(\{p_i\}\right)=\sin(\alpha)\sin(\beta)+\sin\left(\alpha'\right)\sin\left(\beta'\right)-\sum_q p_q\left[\sin\left(\alpha_q\right)\sin\left(\beta_q\right)+\sin\left(\alpha_s\right)\sin\left(\beta_s\right)\right]$, respectively. It is noted that the farfield approximation is explicitly used in the second line of **Eq. C8**. It is readily observed from **Eq. C8** that the parasitic radiation beams can be observed when the vector of $\sum_q p_q\left(\hat{\boldsymbol{r}}_q+\hat{\boldsymbol{r}}_s\right)+\hat{\boldsymbol{r}}+\hat{\boldsymbol{r}}$ is perpendicular to the normal of the one-bit coding metasurface, and these unwanted parasitic beams are described by the perturbation terms of **Eq. C4** :

$$B_1^{SIMO}\exp\left(-j\phi_q\right)A_{\{p_i\}}^{SIMO}\left(r,\boldsymbol{r}';\{q\},s\right),(q=1,2,\ldots,Q).$$

Discussion 4. The efficiency of the closed-form expression $\mathcal{C}_{m,n}^{SIMO}$

As an additional set of examinations for **Figs. 4** and **5** in the main text, we validate our closed-form solution in designing the desired radiation pattern of the one-bit coding metasurface. As an illustrative example, we consider the SIMO case with Q = 3, and thus $\mathcal{C}_{m,n}^{SIMO}$ is concerned. To this end, we study the performance of the modified Gerchberg-Saxton (G-S) algorithm [32] initialized with the result by $\mathcal{C}_{m,n}^{SIMO}$. **Figure C1(a)** plots the evolution behavior of the intensities at three intended receivers with growing iteration. **Figure C1(b)** show spatial maps of $\left|\widehat{\mathcal{H}}_{\mathrm{SISO}}\right|$ of the onebit coding metasurface for three different iteration steps (iteration=1,5 and 10). Note that the result of $\left|\widehat{\mathcal{H}}_{SISO}\right|$ with iteration=1 is just the result using our formula $\mathcal{C}_{m,n}^{SIMO}$. This set of figures show that no obvious improvement is observed by using the iterative GS algorithm when it is initialized by our simple formula. That is to say, the proposed formula for obtaining the coding pattern of the one-bit coding metasurface, $\mathcal{C}_{m,n}^{SIMO}$, yields satisfactory results of a quality comparable to that achieved with the iterative G-S algorithm.

Discussion 5. Approximating the system response of the continuous metasurface with that of a one-bit coding metasurface

We investigate the relation of the system response between the ideal and one-bit coding metasurface from the viewpoint outlined by **Eq. 8** in main text. For illustrative purposes, we here consider the SIMO case. **Figure C2(a)** reports the map of the approximate error (relative RMSE) for varying Q and K. A red dash-dotted line indicates the contour on which the relative RMSE is 0.2. We denote with $K_{0.2}(Q)$ the value of K at a given Q for which the relative RMSE is 0.2. In **Figure C2(b)**, we compare the dependence of $K_{0.2}$ and $Q/\gamma_{\text{one-bit}}$ on the number of channels Q. It is clear that the system response of the ideal metasurface can be well approximated by using K responses of the one-bit coding metasurface which can be achieved by using one one-bit programmable metasurface with K well-designed control coding patterns.

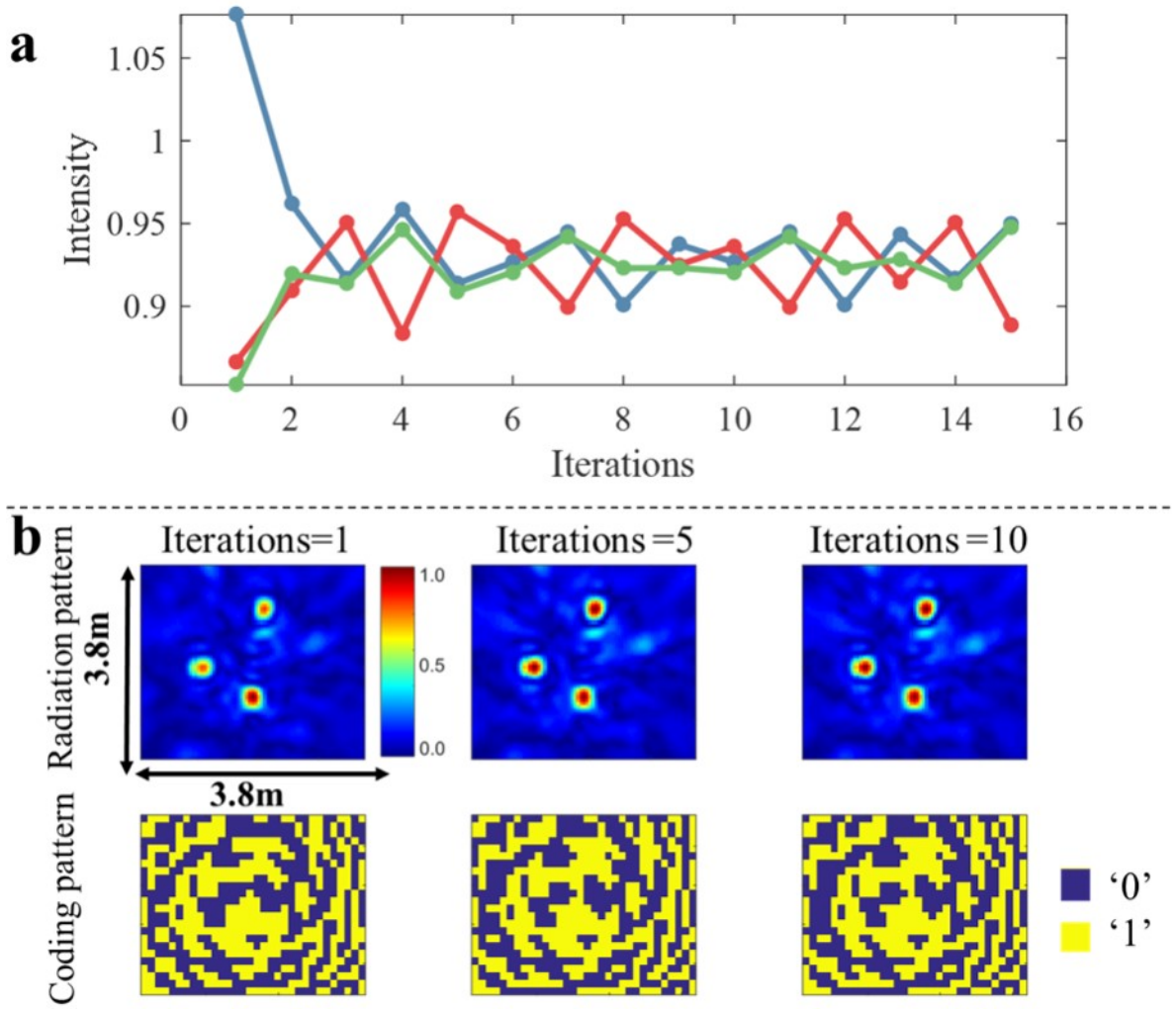

Figure C1 **a**. The evolution behavior of the intensities at three intended receivers with the growth of iteration. **b**. Spatial maps of $\left|\widehat{\mathcal{H}}_{\mathrm{SISO}}\right|$ for three different iteration steps, i.e., iteration=1,5 and 10. Note that the result of $\left|\widehat{\mathcal{H}}_{SISO}\right|$ with iteration=1 is just the result by using our formula $\mathcal{C}_{m,n}^{SIMO}$. Here, the resultant coding patterns of the one-bit coding metasurface have also been provided.

Appendix D Derivation of the MIMO's system response

We here elaborate on the derivation of the MIMO's system response of the one-bit metasurface. In this case, the coding pattern of the one-bit coding pattern reads:

$$\mathcal{C}_{m,n}^{MIMO} = \mathrm{sign}\left[\sum_{s=1}^{S}\sum_{q_s=1}^{Q_s}\cos\left(\tilde{\phi}_{nm}^{MIMO}\left(q_s\right)\right)\right] \tag{D1}$$

where $\tilde{\phi}_{nm}^{MIMO}\left(q_s\right) \equiv \tilde{\phi}_{m,n}\left(\boldsymbol{r}_q;\boldsymbol{r}_s\right), \tilde{\phi}_{m,n}\left(\boldsymbol{r}_q;\boldsymbol{r}_s\right) = \Delta_{m,n}\left(\boldsymbol{r}_q;\boldsymbol{r}_s\right) + \phi_{q_s}$, and $\Delta_{m,n}\left(\boldsymbol{r}_q;\boldsymbol{r}_s\right) = k(\underbrace{|\boldsymbol{r}_s - \boldsymbol{r}_{m,n}|}_{R_{nm}(r_s)} + \underbrace{|\boldsymbol{r}_q - \boldsymbol{r}_{m,n}|}_{R_{nm}(r_q)})$.

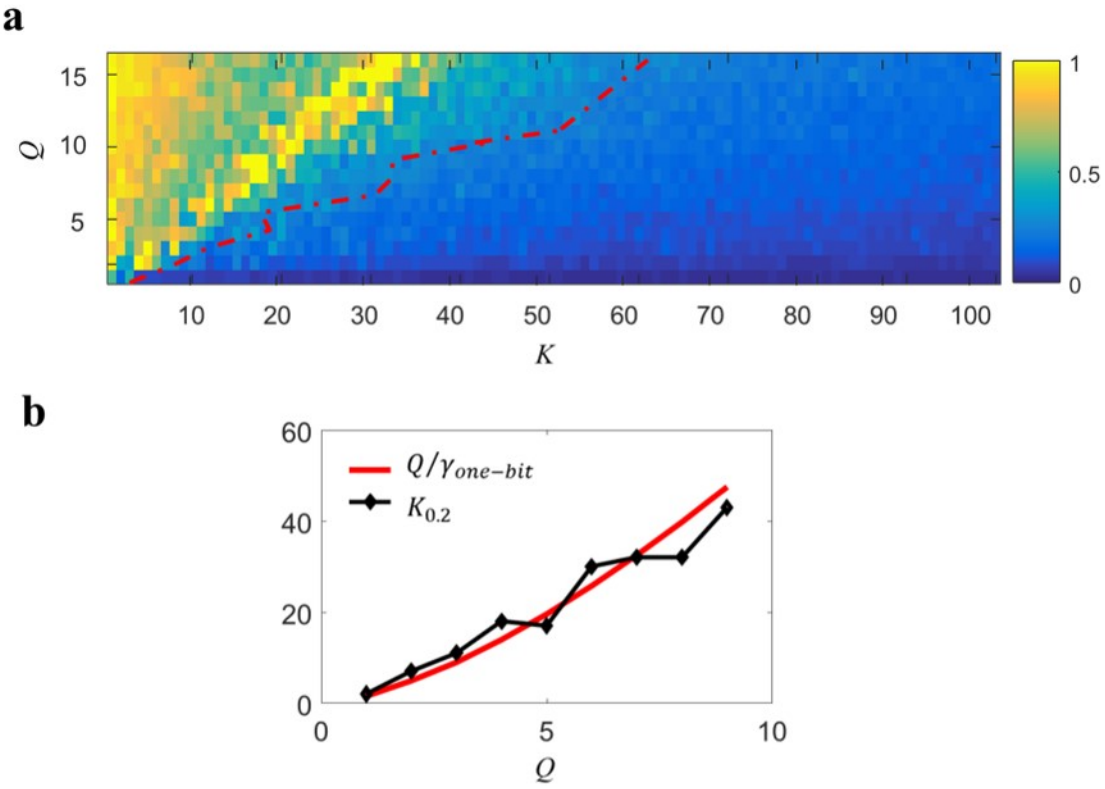

Figure C2 The relation of the system responses for continuous and one-bit coding metasurfaces. **a**. Map of relative RMSE using K well-designed system responses of the one-bit coding metasurface to approximate that of the continuous coding metasurface. The red line indicates the contour at which the relative RMSE is 0.2. **b**. Comparison of the dependence of $K_{0.2}$ and $Q/\gamma_{\text{one-bit}}$ on the number of channels Q.$K_{0.2}$ denotes the value of K when the approximate RMSE is 0.2 (see red dash-dotted line in **a**.

Along the same line as that in Appendix **A** and **C**, we can express **Eq. D1** as follows

$$
\begin{aligned}
\mathcal{C}_{m,n}^{SIMO} &= \operatorname{sign}\left[\sum_{s=1}^{S}\sum_{q_s=1}^{Q_S}\cos\left(\tilde{\phi}_{nm}^{MIMO}\right)\right] = \frac{-j}{\pi}\int_{-\infty}^{\infty}\frac{1}{\xi}\prod_{s=1}^{S}\prod_{q_s=1}^{Q_S}\exp\left[j\xi\cos\left(\tilde{\phi}_{m,n}\right)\right]d\xi \\
&= \frac{-j}{\pi}\int_{-\infty}^{\infty}\frac{1}{\xi}\sum_{\{p_{q_s}\}} j^{\sum_{\{q_s\}} p_{q_s}}\exp\left(j\sum_{\{q_s\}} p_{q_s}\tilde{\phi}_{nm}\right)\prod_{\{q_s\}} J_{p_{q_s}}(\xi)d\xi \\
&= \sum_{\{p_{q_s}\}}\exp\left(j\sum_{\{q_s\}} p_{q_s}\tilde{\phi}_{nm}\right)\underbrace{\frac{-j}{\pi}\int_{-\infty}^{\infty}\frac{1}{\xi}j_{\{q_s\}}p_{q_s}\prod_{\{q_s\}} J_{p_{q_s}}(\xi)d\xi}_{B_{\{q_{q_s}\}}^{MiMO}} \\
&= \sum_{\{p_{q_s}\}} B_{\{p_{q_s}\}}^{MIMO}\exp\left(j\sum_{\{q_s\}} p_{q_s}\tilde{\phi}_{nm}\right)
\end{aligned}
\tag{D2}
$$

Herein, $\sum_{\{p_{q_s}\}} \equiv \underbrace{\sum_{p_{1_1}}\sum_{p_{2_1}}\cdots\sum_{Q_{Q_1}}}_{s=1}\underbrace{\sum_{p_{1_2}}\sum_{p_{2_2}}\cdots\sum_{p_{Q_2}}}_{s=2}\cdots\underbrace{\sum_{p_{1_S}}\sum_{p_{2_S}}\cdots\sum_{p_{Q_S}}}_{s=s}$, $\sum_{p_{q_s}} = \sum_{q_{q_s}=-\alpha}^{\alpha}$, $\sum_{\{q_s\}} \equiv \sum_{s=1}^{S}\sum_{q_s=1}^{Q_s}$,and $\prod_{\{q_s\}} \equiv$

$\prod_{s=1}^{S}\prod_{q_s=1}^{Q_s}$. Then the MIMO's system response of the one-bit coding metasurface can be derived as

$$\begin{aligned}
&\widehat{\mathcal{H}}_{\text{MIMO}}\ (\mathbf{r},\mathbf{r}';\{q_s\}) = \sum_{m,n}\mathcal{C}_{m,n}^{MIMO}\frac{\exp\left[-j\Delta_{nm}\left(r;\mathbf{r}'\right)\right)]}{R_{nm}(\mathbf{r})R_{nm}\left(\mathbf{r}'\right)}\\
&= \sum_{\{p_{q_s}\}}\exp\left(j\sum_{\{q_s\}}p_{q_s}\phi_{q_s}\right)B_{\{q_{q_s}\}}^{MIMO}\underbrace{\sum_{m,n}\frac{\exp\left[j\sum_{q_s}p_{q_s}\Delta_{m,n}\left(r_q;r_s\right)-j\Delta_{nm}\left(r;\mathbf{r}'\right)\right)\right]}{R_{nm}(r)R_{nm}\left(\mathbf{r}'\right)}}_{A_{\{p_{q_s}\}}^{MIMO}(r,\mathbf{r}';\{p_{q_s}\})}\\
&= \sum_{\{p_{q_s}\}}\exp\left(j\sum_{\{q_s\}}p_{q_s}\phi_{q_s}\right)\underbrace{A_{\{q_s\}}^{MI}\left(\boldsymbol{r},\mathbf{r}'\right)B_{\{p_s\}}^{MIMO}}_{A_{\{p_{q_s}\}}^{MIMO}(r,\mathbf{r}'\{\{q_s\})}}
\end{aligned}\tag{D3}$$

Now, the derivation of the MIMO's system response of the one-bit coding metasurface is completed, i.e.,

$$\begin{aligned}
\widehat{\mathcal{H}}_{MIMO}\left(\boldsymbol{r},\mathbf{r}';\{q_s\}\right) &= \underbrace{E_{1\ \text{MIMO}}\ \left(\boldsymbol{r},\mathbf{r}';\{q_s\}\right)}_{\text{leading term}}\\
&+\underbrace{\sum_{\{p_{q_s}\}/\left\{\sum_{\{q_s}|p_{q_s}|=1\&p_{\ q_s\neq -1\}}E_{\{q_s\}}^{MIMO}\left(\boldsymbol{r},\mathbf{r}';\{q_s\}\right)\exp\left[j\sum_{s=1}^{S}\sum_{q_s=1}^{Q_s}p_{q_s}\phi_{q_s}\right]}_{\text{perturbation terms}}
\end{aligned}\tag{D4}$$

where $E_1^{MIMO}\left(\boldsymbol{r},\mathbf{r}';\{q_s\}\right)=B_1^{MIMO}\sum_{s=1}^{S}\sum_{q_s=1}^{Q_s}\exp\left(j\phi_{q_s}\right)A_1^{SISO}\left(\boldsymbol{r},\mathbf{r}';q,s\right)$. In addition, the operator $\sum_{\left\{p_{q_s}\right\}/\left\{\sum_{\{q_s]}|p_{q_s}|=1\&p_{q_s}\neq -1\right\}}$ is defined similar to that of **Eq .C4**.

Discussion 1. Derivation of $B_{\{p_{qs}\}}^{MIMO}$ for the double-input double output case.

Here, we briefly discuss the calculation of $B_{\{p_{qs}\}}^{MIM}$ for a special case of S = 2 and $Q_1 = Q_1 = 1$. In this case, the closed-form solution of $B_{\{p_{q_s}\}}^{MIMO}$ can obtained:

$$B_{\{p_{qs}\}}^{MIMO}=\frac{-j^{(p_1+p_2+1)}}{\pi}\int_{-\infty}^{+\infty}\frac{J_{p_1}(\xi)J_{p_2}(\xi)}{\xi}d\xi=\begin{cases}0, & p_1+p_2\text{ is even}\\ \frac{-j(p_1+p_2+1)}{p_1+p_2}\cdot\left(\frac{2}{\pi}\right)^2\cdot\frac{\sin\left[(p_1-p_2)\frac{\pi}{2}\right]}{p_1-p_2}, & p_1+p_2\text{ is odd}\end{cases}$$

and $B_0^{MIMO}=\frac{2}{\pi}\int_0^{\infty}\frac{1}{\xi}J_0(\xi)J_1(\xi)d\xi=\left(\frac{2}{\pi}\right)^2$.

Discussion 2. Parasitic radiation beams of the one-bit coding metasurface

We provide some insights into the parasitic radiation beams when multiple sources and multiple intended receivers are deployed in the far-field region of the one-bit coding metasurface. Similarly, we treat $\sum_{s=1}^{S}\sum_{q_s=1}^{Q_s}p_{q_s}\Delta_{m,n}\left(\boldsymbol{r}_q;\boldsymbol{r}_s\right)-\Delta_{nm}\left(\boldsymbol{r};\boldsymbol{r}'\right)$ as follows:

$$\begin{aligned}
&\sum_{s=1}^{S}\sum_{q_s=1}^{Q_s}p_{q_s}\Delta_{m,n}\left(\boldsymbol{r}_q;\boldsymbol{r}_s\right)-\Delta_{nm}\left(\boldsymbol{r};\boldsymbol{r}'\right)=-\frac{k}{2z}\underbrace{\left(1+\frac{z}{z'}-\sum_{s=1}^{S}\sum_{q_s=1}^{Q_s}p_{q_s}\left(\frac{z}{z_s}+\frac{z}{z_q}\right)\right)}_{\beta^{MIMO}}\rho_{mn}^2\\
&+\frac{k}{z}\underbrace{\left(\rho_x+\frac{z}{z'}\rho_x'-\sum_{s=1}^{S}\sum_{q_s=1}^{Q_s}p_{q_s}\left(\frac{z}{z_s}\rho_{sx}+\frac{z}{z_q}\rho_{qx}\right)\right)}_{b_x^{MIMO}}nd_x\\
&+\frac{k}{z}\underbrace{\left(\rho_y+\frac{z}{z'}\rho_y'-\sum_{s=1}^{S}\sum_{q_s=1}^{Q_s}p_{q_s}\left(\frac{z}{z_s}\rho_{sy}+\frac{z}{z_q}\rho_{qy}\right)\right)}_{b_x^{MIMO}}md_y+k\mathcal{E}^{MIMO}.
\end{aligned}\tag{D5}$$

Herein, $\varepsilon^{MIMO}=p\left(z_s+z_q\right)-\left(z'+z\right)+\sum_{s=1}^{S}\sum_{q_s=1}^{Q_s}p_{q_s}\left(\frac{\rho_s^2}{2z_s}+\frac{\rho_q^2}{2z_q}\right)-\left(\frac{\rho'^2}{2z'}+\frac{\rho^2}{2z}\right)$. Then, the closed-form solution of $A_{\{p_{q_s}\}}^{MIMO}\left(\boldsymbol{r},\mathbf{r}',\{q_s\}\right)$ can be derived as:

$$\begin{aligned}
A_{\{p_{q_s}\}}^{MIMO}\left(\boldsymbol{r},\boldsymbol{r}'\right)&=\sum_{m,n}\frac{\exp\left(j\left[\sum_{s=1}^{S}\Sigma_{q_s=1}^{Q_s}p_{\ q_s\Delta_{m,n}(r_q;\boldsymbol{r}_s)-\Delta_{m,n}(r;r')}\right]\right)}{R_{nm}(r)R_{nm}\left(r'\right)}\\
&\approx\frac{1}{zz\prime}\frac{\pi}{\alpha+i\frac{k\beta^{MIMO}}{2z}}\exp\left(-\frac{k^2}{4Z^2}\frac{\left(b_x^{MIMO}\right)^2+\left(b_y^{MIMO}\right)^2}{\alpha+i\frac{k\beta^{MIMO}}{2z}}\right)\exp\left(jk\varepsilon^{MIMO}\right).
\end{aligned}\tag{D6}$$

From the above expression, we note that the parasitic radiation beams can be observed at $\left(\rho_x\left(\{p_{q_s}\}\right),\rho_y\left(\{p_{q_s}\}\right),z\right)$, where $\rho_x\left(\{p_{q_s}\}\right)=\sum_{s=1}^{S}\sum_{q_s=1}^{Q_s}p_{q_s}\left(\frac{z}{z_s}\rho_{sx}+\frac{z}{z_q}\rho_{qx}\right)-\frac{z}{z'}\rho_x'$, and $\rho_y\left(\{p_{q_s}\}\right)=\sum_{s=1}^{S}\sum_{q_s=1}^{Q_s}p_{q_s}\left(\frac{z}{z_s}\rho_{sy}+\frac{z}{z_q}\rho_{qy}\right)-\frac{z}{z'}\rho_y'$.

Discussion 3. Far-field solution of **Eq. D4**

We study the system response $\widehat{\mathcal{H}}_{\mathrm{MIMO}}$ when the source and intended receivers are in the far-field region of the metasurface. Similar to the SIMO case discussed in **Appendix C**, we deal with $A^{MIMO}_{\{q_s\}}\left(\boldsymbol{r},\mathbf{r}',\{q_s\}\right)$ as follows

$$\begin{aligned}
A^{MIO}_{\{q_{q_s}\}}\left(\boldsymbol{r},\boldsymbol{r}';\{q_s\},s\right) &\approx \frac{\exp\left[jk\sum_{q_s}p_{q_s}\left(r_{q_s}+r_s\right)-jk\left(\left(r+r'\right)\right)\right]}{rr'} \\
&\times\sum_{m,n}\exp\left[-jk\boldsymbol{r}_{m,n}\cdot\sum_{q_s}p_{q_s}\left(\hat{\boldsymbol{r}}_q+\hat{\boldsymbol{r}}_s\right)+jk\boldsymbol{r}_{m,n}\cdot\left(\hat{\boldsymbol{r}}+\hat{\boldsymbol{r}}'\right)\right] \\
&\approx -\frac{\exp\left[jk\sum_{q_s}p_{q_s}\left(r_q+r_s\right)-j\left(\left(r+r'\right)\right)\right]}{rr'} \\
&\times L_xL_y\,\mathrm{sinc}\left(\frac{1}{2}kL_x\xi^{MIMO}\left(\{q_s\}\right)\right)\mathrm{sinc}\left(\frac{1}{2}kL_y\eta^{MIMO}\left(\{q_s\}\right)\right)
\end{aligned} \tag{D7}$$

Herein, ξ^{MIMO} and η^{MIMO} are defined as:

$$\begin{aligned}
\xi^{MIMO}\left(\{p_{q_s}\}\right) &= \sin(\alpha)\cos(\beta)+\sin\left(\alpha'\right)\cos\left(\beta'\right) \\
&\quad-\sum_{q_s}p_{q_s}\left[\sin\left(\alpha_{q_s}\right)\cos\left(\beta_{q_s}\right)+\sin\left(\alpha_s\right)\cos\left(\beta_s\right)\right] \\
\eta^{MIMO}\left(\{p_{q_s}\}\right) &= \sin(\alpha)\sin(\beta)+\sin\left(\alpha'\right)\sin\left(\beta'\right) \\
&\quad-\sum_{q_s}p_{q_s}\left[\sin\left(\alpha_{q_s}\right)\sin\left(\beta_{q_s}\right)+\sin\left(\alpha_s\right)\sin\left(\beta_s\right)\right].
\end{aligned}$$

From **Eq. D7**, the parasitic radiation beam is observed when the vector of $\sum_{q_s}p_{q_s}\left(\hat{\boldsymbol{r}}_q+\hat{\boldsymbol{r}}_s\right)+\hat{\boldsymbol{r}}+\hat{\boldsymbol{r}}'$ is perpendicular to the normal of the one-bit coding metasurface.

Appendix E Derivation of Eq. 9

We here detail the derivation of **Eq. 9** in the main text. In terms of the definition of statistical coherence, we arrive at

$$\begin{aligned}
\left\langle\widehat{\mathcal{H}}_{SIMO}\left(\boldsymbol{r}_i\right),\widehat{\mathcal{H}}_{SIMO}\left(\boldsymbol{r}_j\right)\right\rangle &= \left|\mathrm{B}_0\right|^2\sum_{q=1}^{Q}\sum_{q'=1}^{Q}A_q\left(\boldsymbol{r}_i\right)A^*_{q'}\left(\boldsymbol{r}_j\right)\left\langle\exp\left(j\left(\phi_q-\phi_{qq'}\right)\right)\right\rangle \\
&+\mathrm{B}_0\sum_{q=1}^{Q}A_q\left(\boldsymbol{r}_i\right)\sum_{p_{i:1\to Q}}E^*_{\{p_i\}}\left(\boldsymbol{r}_j\right)\left\langle\exp\left[j\phi_q-j\sum_{q'=1}^{Q}p_{qq'}\phi_{q'}\right]\right\rangle \\
&+B^*_0\sum_{q=1}^{Q}A^*_q\left(\boldsymbol{r}_j\right)\sum_{p_{i:1\to Q}}E_{\{p_i\}}\left(\boldsymbol{r}_i\right)\left\langle\exp\left[j\sum_{qq'=1}^{Q}p_{qq'}\phi_{q'}-j\phi_q\right]\right\rangle \\
&+\sum_{p_{i:1\to Q}}\sum_{p'_i:1\to Q}E_{\{p_i\}}\left(\boldsymbol{r}_i\right)E^*_{\{p'_i\}}\left(\boldsymbol{r}_j\right)\left\langle\exp\left[j\sum_{q=1}^{Q}\left(p_q-p'_q\right)\phi_q\right]\right\rangle
\end{aligned} \tag{E1}$$

Taking the following identical equations into account, namely,

$$\begin{aligned}
&\left\langle\exp\left(j\left(\phi_q-\phi_{q'}\right)\right)\right\rangle=\delta_{q-q'}, \\
&\left\langle\exp\left[j\sum_{q'=1}^{Q}p_{q'}\phi_{q'}-j\phi_q\right]\right\rangle=\delta_{p_q-1-nM_q}\prod_{q'=1,q'\neq q}^{Q}\delta_{p_{q'}-nM_{q'}}, \\
&\left\langle\exp\left[j\sum_{q=1}^{Q}\left(p_q-p'_q\right)\phi_q\right]\right\rangle=\prod_{q=1}^{Q}\delta_{p_q-p'_q-nM_q},
\end{aligned}$$

we can rewrite **Eq. E1** as:

$$\begin{aligned}
\left\langle\widehat{\mathcal{H}}_{SIMO}\left(\boldsymbol{r}_i\right),\widehat{\mathcal{H}}_{SIMO}\left(\boldsymbol{r}_j\right)\right\rangle &= \left|\mathrm{B}_0\right|^2\sum_{q=1}^{Q}A_q\left(\boldsymbol{r}_i\right)A^*_q\left(\boldsymbol{r}_j\right) \\
&+\mathrm{B}_0\sum_{q=1}^{Q}A_q\left(\boldsymbol{r}_i\right)\sum_{n_{i:1\to Q/n}}E^*_{\{M_in_i\}}\left(\boldsymbol{r}_j\right) \\
&+B^*_0\sum_{q=1}^{Q}A^*_q\left(\boldsymbol{r}_j\right)\sum_{n_{i:1\to Q/n_q}}E_{\{M_in_i\}}\left(\boldsymbol{r}_i\right) \\
&+\sum_{p_{i:1\to Q}}\sum_{p'_i:1\to Q}E_{\{p_i\}}\left(\boldsymbol{r}_i\right)E^*_{\{p'_i\}}\left(\boldsymbol{r}_j\right)\prod_{q=1}^{Q}\delta_{p_q-p'_q-nM_q}
\end{aligned} \tag{E2}$$

Herein, we have introduced the following notation

$$\sum_{n_{i:1\to Q/n_q}}\equiv\sum_{n_1=-N,}^{N},\cdots\sum_{n_{q-1}=-N}^{N}\sum_{n_q=-N+1/M_q}^{N+1/M_q}\sum_{n_{q+1}=-N}^{P}\cdots\sum_{n_Q=-N}^{N}$$

We here consider a more realistic scenario that two receivers are well separated in terms of the Rayleigh limit, i.e., $|A_q(\boldsymbol{r}_i)| \approx 0$ for $i \neq q$. Then, **Eq. E2** reads:

$$\begin{aligned}\left\langle \widehat{\mathcal{H}}_{SIMO}(\boldsymbol{r}_i), \widehat{\mathcal{H}}_{SIMO}(\boldsymbol{r}_j) \right\rangle \approx & \mathrm{B}_0 A_i(\boldsymbol{r}_i) \sum_{\frac{n_{i:1\to Q}}{n_q}} E^*_{\left\{M_i n_{i\}\right.}}(\boldsymbol{r}_j) \\ & + B_0^* A_j^*(\boldsymbol{r}_j) \sum_{n_{i:1\to Q}/n_q} E_{\left\{M_i n_i\right\}}(\boldsymbol{r}_i), \quad \text{for } i \neq j\end{aligned}$$

$$\begin{aligned}\left\langle \widehat{\mathcal{H}}_{SIMO}(\boldsymbol{r}_i), \widehat{\mathcal{H}}_{SIMO}(\boldsymbol{r}_i) \right\rangle = & |\mathrm{B}_0 A_0|^2 + \mathrm{B}_0 A_i(\boldsymbol{r}_i) \sum_{n_{i:1\to Q}/n_q} E^*_{\left\{M_i n_i\right\}}(\boldsymbol{r}_j) \\ & + B_0^* A_i^*(\boldsymbol{r}_i) \sum_{n_{i:1\to Q}/n_q} E_{\left\{M_i n_i\right\}}(\boldsymbol{r}_i)\end{aligned}$$

Now, the derivation of **Eq. 10** in the main text is completed.

Appendix F Derivation of Eq. 10

We provide briefly the derivation of **Eq. 10** in the main text. Along the same line as that in **Appendix E**, we can arrive at the expressions of μ_u^{SIMO} and σ_u^{SIMO}

$$\begin{aligned}\mu_u^{\mathrm{SIMO}} &= \left\langle \widehat{\mathcal{H}}_{SIMO}(\boldsymbol{r}_u, \boldsymbol{r}_s; \{q\}, s) \right\rangle \\ &= \mathrm{A}_0\ \mathrm{B}_0 \exp(j\phi_i) + \sum_{p_{i:1\to Q}} \left(E_{\left\{p_i\right\}}(\boldsymbol{r}_i) \exp[j p_i \phi_i] \prod_{q=1, q\neq i}^{Q} \delta_{p_q - nM_q} \right)\end{aligned} \tag{F1}$$

$$\begin{aligned}\sigma_u^{SIMO} &= \left\langle \left| \widehat{\mathcal{H}}_{SIMO}(\boldsymbol{r}_u, \boldsymbol{r}_s; \{q\}, s) - \left\langle \widehat{\mathcal{H}}_{SIMO}(\boldsymbol{r}_u, \boldsymbol{r}_s; \{q\}, s) \right\rangle \right|^2 \right\rangle \\ &= |\mathrm{B}_0|^2 \sum_{q=1, q\neq i}^{Q} \sigma_q^2 \lfloor A_q(\boldsymbol{r}_i) \rceil^2 + \chi(\{M_q\}),\end{aligned} \tag{F2}$$

in which,

$$\begin{aligned}\chi(\{M_q\}) &\equiv \sum_{\left\{p_{i/nM_i}\right\}} \sum_{\left\{p_i'/nM_i\right\}} E_{\left\{p_i\right\}}(\boldsymbol{r}_i) E^*_{\left\{p_i'\right\}}(\boldsymbol{r}_i) \exp\left[j\left(p_i - p_i'\right)\phi_i\right] \prod_{q=1}^{Q} \delta_{p_q - p_q' - nM_q} \\ &\leqslant \sum_{\left\{p_{i/nM_i}\right\}} \sum_{\left\{p_i'/nM_i\right\}} \left| E_{\left\{p_i\right\}}(\boldsymbol{r}_i) E^*_{\left\{p_i'\right\}}(\boldsymbol{r}_i) \right| \prod_{q=1}^{Q} \delta_{p_q - p_q' - nM_q}\end{aligned} \tag{F3}$$

wherein

$$\sum_{\left\{p_i'/nM_i\right\}} \equiv \sum_{\substack{p_1=-P, \\ p_1\neq nM_1,}}^{P} \cdots \sum_{p_{q-1}=-P, p_{q-1}\neq nM_{q-1}}^{P} \sum_{p_q=-P}^{P} \sum_{p_{q+1}=-P, p_{q+1}\neq nM_{q+1}}^{P} \cdots \sum_{\substack{p_Q=-P. \\ p_Q\neq nM_Q}}^{P}$$

Appendix G Discussions on Fig. 3

In **Fig.H1(a)** and **H2(c)**, we report the dependence of $\Delta\varphi_{\mathrm{SISO}}(\boldsymbol{r}_q)$ on $\boldsymbol{r}_q$ for QPSK ($M_q = 4$) with the incident source deployed at $(0, 0, 2\ \mathrm{m})$ and $(0, 1.15\ \mathrm{m}, 2\ \mathrm{m})$, respectively. We note that the source is deployed in the near-field region of the metasurface. Correspondingly, the dependences of EC^{SISO} on $\boldsymbol{r}_q$ are also provided in **Fig. H1(b)** and **H2(d)**, respectively. It can be observed from this set of results that the one-bit coding metasurface has the ability to perform the QPSK information encoding with high fidelity within the whole observation region.

We next examine the ability of the one-bit coding metasurface to perform PSK information encoding by varying its scale. **Figure H2** shows the results for the case of 16-level PSK, where the simulation setup is the same as that in **Fig. 3c** in the main text. More specifically, **Figs. H2(b-d)** present the dependence of the half-power-beam-width (HPBW), the beam scanning error, and the ratio of the leading term to the perturbation terms of the radiation beam on the metasurface size for four selected locations $\boldsymbol{r}_q$ marked with (1) (2) (3) and (4) in **Fig. H2(a)**. From this set of figures, we observe that the performance of the one-bit coding metasurface in manipulating the beam and associated information can be efficiently improved by increasing the aperture of metasurface.

Appendix H Bit error analysis

We give the analysis on bit error rate (BER) for the one-bit coding metasurface. For discussion convenience, several notations are introduced. With loss of generality, we consider the wireless channel for transferring digital information with M-level phase shift key (MPSK) modulation, and use the Bayesian decision rule for information retrieval. With reference to Supplementary Figure S1, for the i th information symbol, the intended phase is μ_i, the biased mean phase is θ_i due to the one-bit quantization of the coding metasurface, and the total noise level (the conventional system noise plus the one-bit-quantization noise) is σ_i^2. Then, BER in total reads

$$BER = 1 - \sum_{i=1}^{M} \int_{2\pi(i-1)/M}^{2\pi i/M} \frac{1}{\sqrt{2\pi}\sigma_i} \exp\left(-\frac{(x - \theta_i - \mu_i)^2}{2\sigma_i^2} \right) dx \tag{H1}$$

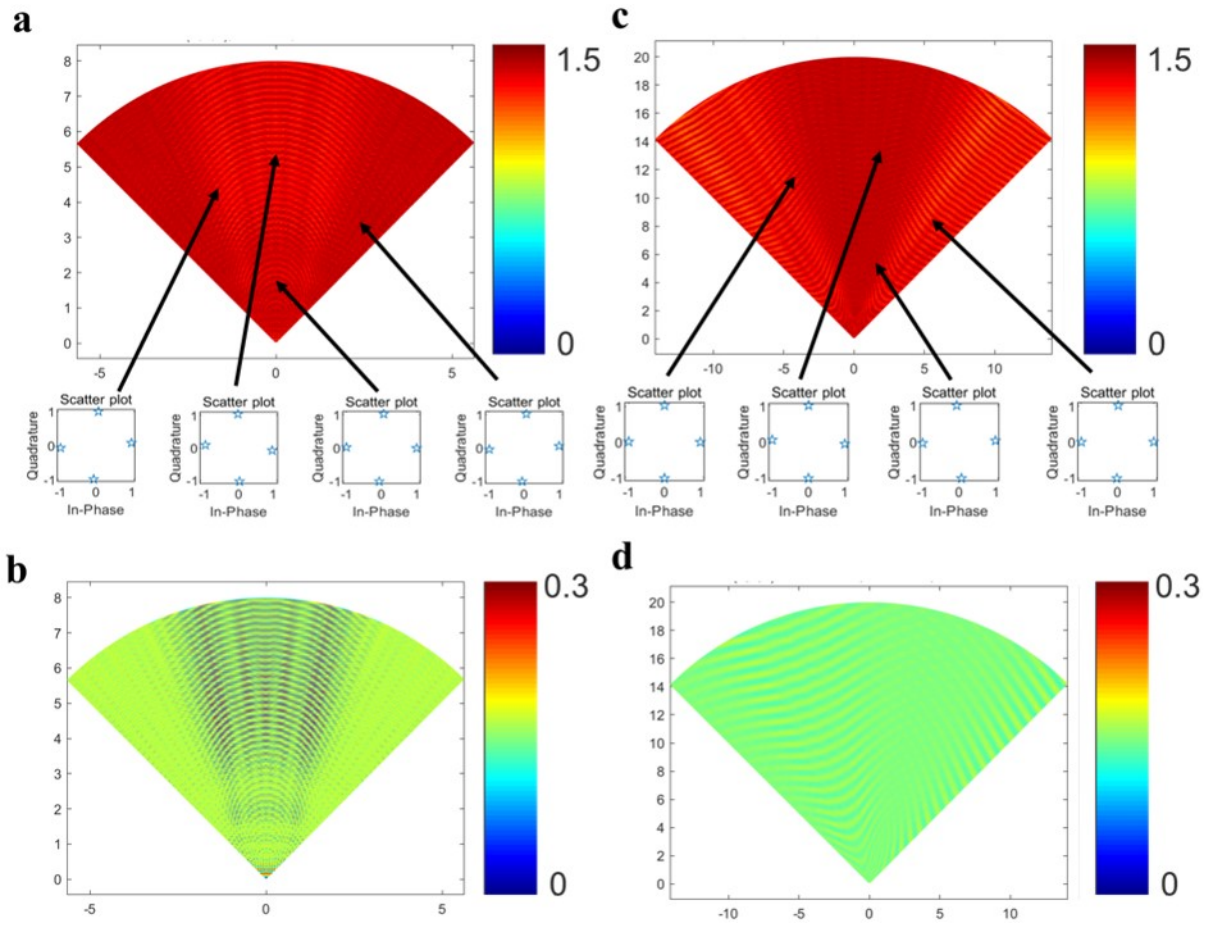

Figure H1 QPSK with the one-bit coding metasurface in SISO when the source is deployed in the near-field region of the metasurface. **a,c.** Dependence of phase resolution $\Delta\varphi_{\mathrm{SISO}}$ on the receiver's location $\boldsymbol{r}_q$. Considered receiver locations are within a distance between 0 and 20 m from the metasurface for azimuth between -60° and 60°. The insets provide representative constellation diagrams. Different levels of PSK and source locations are considered, as indicated in the subfigure titles. The source is deployed at $(0, 0, 2$ m) in **a**, while $(0, 1.3$ m$, 2$ m) in **c**. **b,d.** Dependence of EC^{SISO} on $\boldsymbol{r}_q$ for the same settings as in **a** and **c**.

Figure 7 in the main text shows the dependence of BER on M with system SNR of 20 dB, where the source and receiver are deployed in the near-field region of the one-bit coding metasurface. As a compliment, we consider the performance of the one-bit coding metasurface when the source and receiver are in its far-field region. Figure A6 compares BERs of the one-bit and continuous coding metasurfaces as a function of phase quantization levels in the SISO setting, where the source and receiver are located at $(0, 0, 1$ km) and $(0, 0, 2$ km), respectively. **Fig. H3(a)** shows the dependence of BER on the phase quantization level M in a system with SNR of 20 dB, while **Figs.H3(b)** and **H3(c)** report the constellation diagrams of four-level PSK information phase quantization levels for the continuous and one-bit coding metasurfaces, respectively. The axes are normalized by B_0^{SIMO}. The red-marked and black-marked stars of the constellation diagrams in b and **c** correspond to the system-noise-free case. Notice that the M-PSK ($M > 2$) digital information is degraded to 2-PSK when the one-bit coding metasurface is used. That is to say, the one-bit coding metasurface fails to manipulate the EM information with high-order PSK when the receiver and source are in the blind district.

Appendix I Discussions about non-ideal one-bit quantization of programmable coding metasurfaces

We discuss the system response of the coding metasurface with non-ideal one-bit quantization. Particularly, when the meta-atom is illuminated by a plane wave, its binary response states read:

$$f(x) = \begin{cases} A_+ e^{j\phi_+}, & \text{for state } '1' \\ A_- e^{j\phi_-}, & \text{for state } 0' \end{cases}, \tag{I1}$$

where $0 \leqslant A_+, A_- \leqslant 1$, and $0 \leqslant \phi_+, \phi_- < 2\pi$. Recall the step function denoted by $u(x) = \begin{cases} 1, & x > 0 \\ \frac{1}{2}, & x = 0, \\ 0, & x < 0 \end{cases}$, then the above piece-wise function is expressed as:

$$f(x) = A_+ e^{j\phi_+} u(x) + A_- e^{j\phi_-} u(-x) \tag{I2}$$

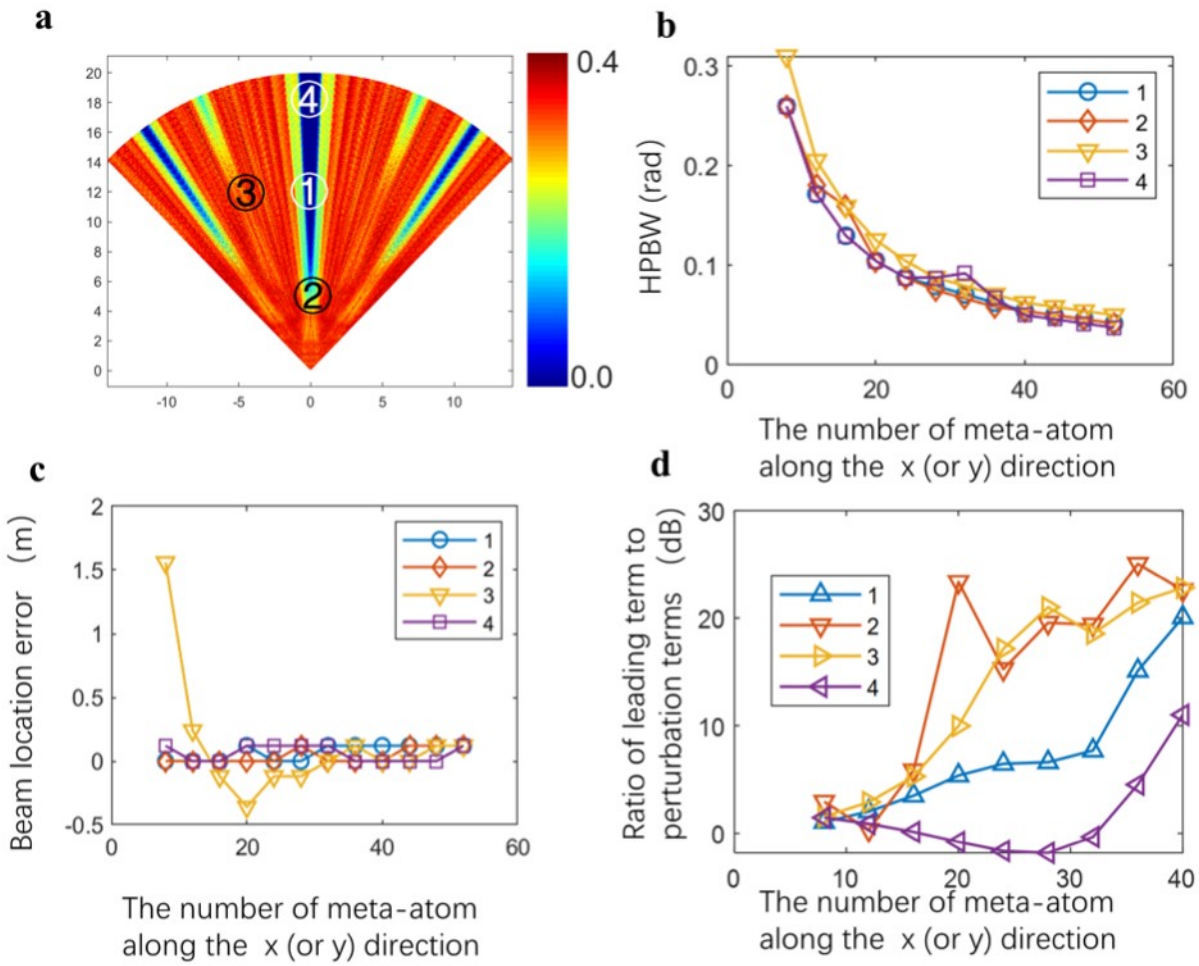

Figure H2 16-level PSK with a one-bit coding metasurface in SISO, where the source is deployed at $(\mathbf{0}, \mathbf{0}, \mathbf{2km})$. **a**. Dependence of phase resolution $\Delta\varphi_{\mathrm{SISO}}$ on the receiver's location $\boldsymbol{r}_q$. Considered receiver locations are within a distance between 0 and 20 m from the metasurface for azimuth between -60° and 60°. **b-d**. Dependence of HPBW, beam scanning error, and ratio of the leading term to the perturbation terms of the radiation beam on the metasurface size for four locations $\boldsymbol{r}_q$ marked with (1) (2) (3) and (4) in **Fig. H2(a)**, respectively.

Immediately, **Eq. I2** can be further expressed as

$$\begin{aligned} f(x) &= \frac{\left(A_+ e^{j\phi_+ + A_- e^{j\phi_-}}\right)}{2} + \frac{\left(A_+ e^{j\phi_+ - A_- e^{j\phi_-}}\right) e^{-j\pi/2}}{2\pi} \int_{-\infty}^{\infty} \frac{\exp(jx\xi)}{\xi} d\xi \\ &= \frac{\left(A_+ e^{j\phi_+ + A_- e^{j\phi_-}}\right)}{2} + \frac{\left(A_+ e^{j\phi_+ - A_- e^{j\phi_-}}\right)}{2} \cdot \frac{-j}{\pi} \int_{-\infty}^{\infty} \frac{\exp(jx\xi)}{\xi} d\xi \end{aligned} \tag{I3}$$

It is clear that we have established a simple relation of the responses between the ideal one-bit meta-atom and non-ideal meta-atom. As a result, for the non-ideal one-bit coding metasurface, its control coding patterns for SISO, SIMO and MIMO can be derived as:

$$\mathcal{C}_{m,n}^{\text{non-ideal,SISO}} = \gamma_0 + \gamma_1 \mathcal{C}_{m,n}^{SISO}, \tag{I4a}$$

$$\mathcal{C}_{m,n}^{\text{non-ideal,SIMO}} = \gamma_0 + \gamma_1 \mathcal{C}_{m,n}^{SIMO}, \tag{I4b}$$

$$\mathcal{C}_{m,n}^{\text{non-ideal,MIMO}} = \gamma_0 + \gamma_1 \mathcal{C}_{m,n}^{MIMO}. \tag{I4c}$$

For SISO, SIMO and MIMO, the system responses of the coding metasurface with the non-ideal one-bit quantization can be readily derived as:

$$\widehat{\mathcal{H}}_{\text{SISO}}^{\text{non-idea}} \left(\mathbf{r}, \mathbf{r}'; q, s\right) = \gamma_0 \sum_{m,n} \frac{\exp\left[-jk\Delta_{nm}\left(r; \mathbf{r}'\right)\right]}{R_{nm}(r) R_{nm}\left(\mathbf{r}'\right)} + \gamma_1 \widehat{\mathcal{H}}_{\text{SISO}} \left(\mathbf{r}, \mathbf{r}'; q, s\right), \tag{I5a}$$

$$\widehat{\mathcal{H}}_{\text{SIMO}}^{\text{non-ideal}} \left(\mathbf{r}, \mathbf{r}'; \{q\}, s\right) = \gamma_0 \sum_{m,n} \frac{\exp\left[-jk\Delta_{nm}\left(\boldsymbol{r}; \mathbf{r}'\right)\right]}{R_{nm}(r) R_{nm}\left(\mathbf{r}'\right)} + \gamma_1 \widehat{\mathcal{H}}_{\text{SIMO}} \left(\mathbf{r}, \mathbf{r}'; \{q\}, s\right), \tag{I5b}$$

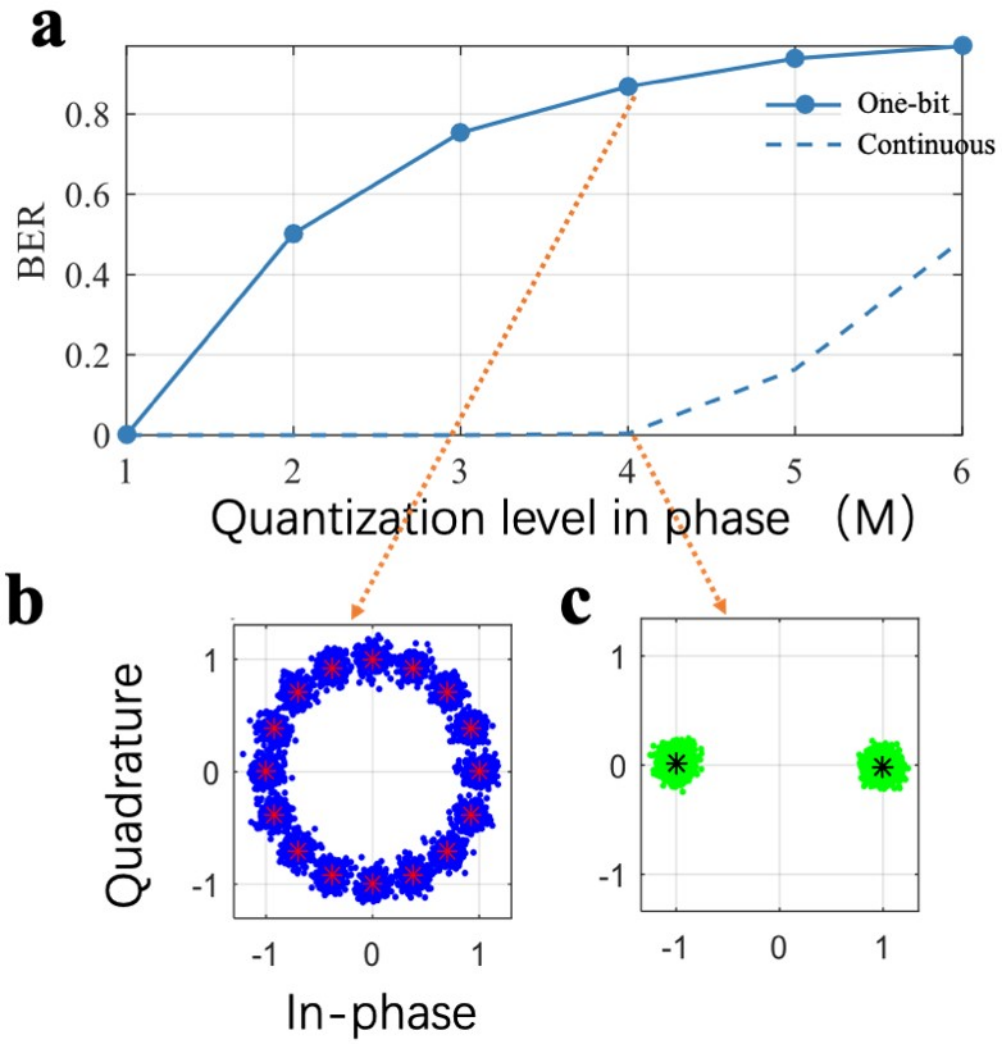

Figure H3 BER comparison of the one-bit and continuous metasurfaces in the SISO setting. **a**. Dependence of BER on the phase quantization level M in a system with SNR of 20 dB, in which the receiver and source are in the "blind district" of the metasurface. The solid and dashed lines represent the cases of continuous and one-bit coding metasurfaces. **b,c**. Constellation diagrams of the 4-PSK phase quantization levels for the continuous and one-bit coding metasurfaces, respectively. The axes are normalized by B_0^{SIMO} . The red-marked and black-marked stars of the constellation diagrams in **b** and **c** correspond to the system-noise-free case.

$$\widehat{\mathcal{H}}_{\mathrm{MIMO}}^{\text{non-ideal}}\left(\mathbf{r},\mathbf{r}';\{q_s\}\right)=\gamma_0\sum_{m,n}\frac{\exp\left[-j\Delta_{nm}\left(r;\mathbf{r}'\right)\right]}{R_{nm}(r)R_{nm}\left(\mathbf{r}'\right)}+\gamma_1\widehat{\mathcal{H}}_{\mathrm{MIMO}}\left(\mathbf{r},\mathbf{r}';\{q_s\}\right). \tag{I5c}$$

We note that the term $\sum_{m,n}\frac{\exp\left[-j\Delta_{nm}\left(r;\mathbf{r}'\right)\right]}{R_{nm}(r)R_{nm}\left(\mathbf{r}'\right)}$ characterizes exactly the conventional Snell's reflection, where the metasurface serves as a perfectly planar reflection mirror. To see it more clearly, we consider the far-field approximation

$$\sum_{m,n}\frac{\exp\left[-jk\Delta_{nm}\left(r;\mathbf{r}'\right)\right]}{R_{nm}(r)R_{nm}\left(\mathbf{r}'\right)}\approx\frac{\exp\left(-jk\left(r+r'\right)\right)}{rr'}\sum_{m,n}\exp\left[jk\boldsymbol{r}_{m,n}\cdot\left(\hat{\boldsymbol{r}}+\hat{\boldsymbol{r}}'\right)\right]\Bigg] \tag{I6}$$

where the following far-field approximation is used:

$$\Delta_{m,n}\left(\boldsymbol{r};\mathbf{r}'\right)=k\left(\left|\mathbf{r}'-\boldsymbol{r}_{m,n}\right|+\left|\boldsymbol{r}-\boldsymbol{r}_{m,n}\right|\right)\approx k\left(r+r'-\boldsymbol{r}_{m,n}\cdot\left(\hat{\boldsymbol{r}}+\hat{\boldsymbol{r}}'\right)\right)$$

Now, it is clear that the term of $\sum_{m,n}\frac{\exp\left[-jk\Delta_{nm}\left(r;\mathbf{r}'\right)\right]}{R_{nm}(r)R_{nm}\left(\mathbf{r}'\right)}$ has a single radiation peak as $\hat{\boldsymbol{r}}=-\hat{\boldsymbol{r}}'$, i.e., the receiver is located in the mirror direction of the source with respect to the normal direction of metasurface. That is to say, the non-ideal one-bit quantization will give rise to the radiation leakage in the mirror direction of the source with respect to the metasurface normal.

Figure H4 shows the dependence of the beam's intensity on the choice of $(\Gamma,\Delta\theta)$ in SISO, where the source is deployed at the location of $(0,0,2$ m), and the map has been normalized with its maximum. Here, Γ and $\Delta\theta$ are defined as: $\Gamma=|A_+|/|A_-|$,

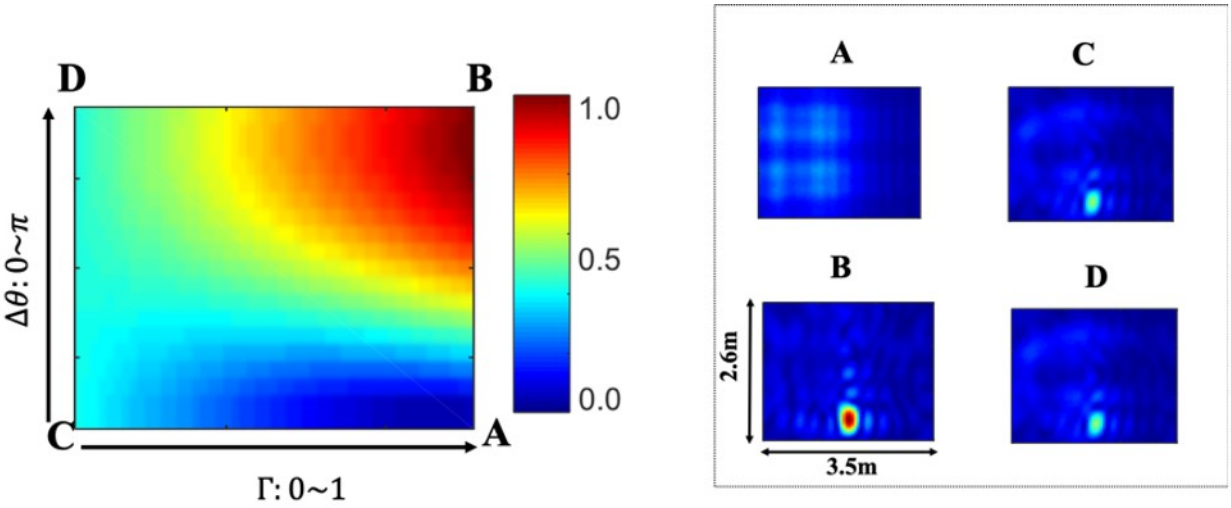

Figure H4 **Figure A7**. Dependence of the beam's intensity on the choice of $(\Gamma, \Delta\theta)$ in SISO. The left: the dependence of beam's intensity on the choice of $(\Gamma, \Delta\theta)$, in which the map has been normalized with its maximum. The right: spatial maps of $\left|\widehat{\mathcal{H}}_{SISO}^{\text{non-ideal}}\right|$ for four selected cases (A: $\Gamma = 1,\ \Delta\theta = 0$; B : $\Gamma = 1, \Delta\theta = \pi$; C : $\Gamma = 0, \Delta\theta = \pi$; D : $\Gamma = 0, \Delta\theta = \pi$) marked in the left figure, in which the source is located at $(0, 0, 2$ m) and the observation plane is at the distance of 3 m away from the metasurface.

and $\Delta\theta = \phi_+ - \phi_-$. In addition, we make the assumptions that $|A_-| = 1$ and $\phi_- = 0$. The spatial maps of $\left|\widehat{\mathcal{H}}_{SISO}^{\text{non-ideal}}\right|$ for four representative cases marked in the left of **Fig. H4** are shown in the right of **Fig. H4**. We clearly observe that the one-bit coding metasurface is robust to the non-ideal meta-atoms, in spite of some degraded performance more or less.